[CANCER RESEARCH 64, 8365–8373, November 15, 2004]

Evidence that TRPM8 Is an Androgen-Dependent Ca^{2+} Channel Required for the Survival of Prostate Cancer Cells

Lei Zhang[1] and Gregory John Barritt[2]

[1]Department of Human Physiology and Centre for Neuroscience and [2]Department of Medical Biochemistry, Flinders University, Adelaide, South Australia, Australia

ABSTRACT

The Ca^{2+}-permeable channel TRPM8 is thought to play an important role in the pathophysiology of prostate cancer. We have investigated the intracellular location of TRPM8 and its role as a Ca^{2+}-permeable channel in an androgen-responsive and an androgen-insensitive prostate cancer cell line. We report evidence from immunofluorescence experiments that in the androgen-responsive LNCaP cell line, the TRPM8 protein is expressed in the endoplasmic reticulum and plasma membrane, acts as a Ca^{2+}-permeable channel (assessed using Fura-2 to measure increases in the cytoplasmic Ca^{2+} concentration) in each of these membranes, and is regulated by androgen. Although TRPM8 was detected in the androgen-insensitive PC-3 cell line, no evidence was obtained for regulation of its expression by androgen. The results of experiments using LNCaP cells, the TRPM8 antagonist capsazepine, and small interference RNA targeted to TRPM8 indicate that TRPM8 is required for cell survival. These results indicate that TRPM8 is an important determinator of Ca^{2+} homeostasis in prostate epithelial cells and may be a potential target for the action of drugs in the management of prostate cancer.

INTRODUCTION

Although one of the leading threats to men's health in the Western world (1), there are limited therapeutic options for metastatic prostate cancer. Therefore, it is vital to gain a better understanding of the molecular mechanisms that underlie the development and progression of this disease. It recently has been reported that mRNA encoding TRPM8, a Ca^{2+}-permeable channel belonging to the transient receptor potential family, is expressed in prostate tissues, is greatly upregulated in patients with prostate cancer (2), but is almost lost in the transition to androgen independence and in prostate cancer tissues from patients subjected to preoperative antiandrogen therapy (3). These observations suggest that TRPM8 is an androgen-regulated protein, the loss of which may be associated with advanced stages of the disease. Thus, TRPM8 is a novel prostate cancer biomarker and is likely to play an important role in the pathophysiology of prostate epithelial cells (2, 3). Recent studies of cutaneous ganglion neurons in rat and mouse have shown that orthologues of TRPM8 are functional Ca^{2+}-permeable channels that respond to a cooling stimulus induced by either a decreasing of temperature to $<25°C$ or menthol and icilin (4–7). Electrophysiologic studies of heterologously expressed TRPM8 indicate that it is a ligand-gated nonselective cation channel (P_{Ca}/P_{Na} = 1:3; refs. 4, 5). However, little is known about the function of TRPM8 in prostate tissues. Here we report that in androgen-responsive prostate cancer LNCaP cells, TRPM8 is expressed in the endoplasmic reticulum (ER) and plasma membrane (PM) and acts as a Ca^{2+}-permeable channel in each of these membranes. We also provide evidence that TRPM8 is required for cell survival.

Received 6/17/04; revised 8/28/04; accepted 9/8/04.

The costs of publication of this article were defrayed in part by the payment of page charges. This article must therefore be hereby marked *advertisement* in accordance with 18 U.S.C. Section 1734 solely to indicate this fact.

Requests for reprints: Lei Zhang, Department of Human Physiology, School of Medicine, Faculty of Health Sciences, G.P.O. Box 2100, Adelaide, South Australia, 5001, Australia. Phone: 61-8-8204-8945; Fax: 61-8-8204-5768; E-mail: Lei.zhang@flinders.edu.au.

MATERIALS AND METHODS

Cell Culture and Reverse Transcription-PCR. LNCaP and PC-3 cells were grown in RPMI 1640 plus 5% (v/v) fetal calf serum (FCS), RPMI 1640 plus 5% (v/v) charcoal-stripped FCS (to remove androgens), and RPMI 1640 plus 5% charcoal-stripped FCS plus 5α-dihydrotestosterone (DHT; 0.1 nmol/L) as described previously (8).

Total RNA isolation and reverse transcription were performed using the RNeasy and Ominiscript RT kits (Qiagen, Valencia, CA) following the manufacturer's instructions. The PCR primers (synthesized by Geneworks, Adelaide, Australia) used in the study were TRPM8 (NM_024080; base: 457 to 1138): 5′-GAAAACACCCAACCTGGTCATTTC-3′ (sense): 5′-CACCGTGCGGGGTAAAAAGCG-3′ (antisense); ANKTM1 (NM_007332; base: 1001 to 1412): 5′-TTCATTTTGCTGCCACCCAG-3′ (sense), 5′-CCATCGTTGTCTTCATCCATTACC-3′ (antisense); TRPV1 (AY131289; base: 1755 to 2098): 5′-CGTCTTCTTGTTCGGGTTTTCC-3′ (sense), 5′- GCTTCCAGATGTTCTTGCTCTCC-3′ (antisense); and glyceraldehyde-3-phosphate dehydrogenase (GAPDH; BC023632; base: 527 to 889): 5′-TTGGTATCGTGGAAGGACTC-3′ (sense), 5′-TGCTGTTGAAGTCAGAGGAGAC-3′ (antisense). PCR was conducted (7) using HotStart Taq Master Mix kit (Qiagen) for 20 cycles (GAPDH) and 30 cycles (TRP channels). Initial denaturation was 15 minutes at 95°C and 1 minute at 94°C, followed by a 30-second annealing step at 55°C, 57°C, 55°C, and 56°C for TRPM8, ANKTM1, TRPV1, and GAPDH, respectively, 1-minute elongation at 72°C, and a final elongation of 10 minutes at 72°C. PCR products were analyzed by gel-electrophoresis and DNA sequencing (7). To determine the relative abundance of TRPM8 mRNA, the density of each TRPM8 band (measured using α Imager software; Bio-Rad, Hercules, CA) was compared with that of the respective GAPDH band after background subtraction, and the results are expressed in arbitrary ratio units (aru).

Small Interference RNA Targeted against TRPM8. Small interference RNA (siRNA) targeted against TRPM8 was designed using siRNA Target Finder (Ambion, Inc., Austin, TX), according to the mRNA sequence of human TRPM8 (NM_024088). The TRPM8 siRNA sequence was 5′-AGAAAUUCUCGAAUGUUCUUU-3′ (sense) and 3′-UUUCUUUAAGAGCUUACAAGA-5′ (antisense). The sequence of a negative control siRNA was 5′-UUCUAAUAGGCAUAUUAUCUU-3′ (sense) and 3′-UUAUGAUUAUCCGUAUAAUAG-5′ (antisense). The siRNAs were produced using the *Silence* siRNA Construction Kit (Ambion) following the manufacturer's instructions. Transfection of LNCaP cells with siRNA (20 nmol/L) was conducted by using Lipofectamine 2000 (Invitrogen, Carlsbad, CA) following the manufacturer's instructions. The estimated percentage transfection was $>90\%$.

Identification of Putative Androgen-Response Element Motifs. The 5 kb of genomic sequence upstream of human TRPM8 mRNA sequence and all of its intron sequences (National Center for Biotechnology Information, Bethesda, MD) were used to search for sequences similar to the consensus androgen-response element motif AGAACAnnnTGTTCT (TRANSFAC, Wolfenbüttel, Germany). Scoring was based on the number of nucleotides in the query sequence that matched the consensus sequence using MacVector 7.1 (Accelrys, San Diego, CA). Sequence matches with at least 9 identities of the 12 consensus nucleotides (75%) were taken as showing similarity. All of the putative androgen-response element motifs were aligned using MacVector 7.1 ClustalW (Accelrys; ref. 9).

Immunocytochemistry. Cells were fixed with 4% (w/v) paraformaldehyde, blocked with 20% (v/v) FCS, then incubated with anti-TRPM8 antibody [Abcam, Cambridge, United Kingdom; 1:500 dilution, which detects a single M_r 130,000 band corresponding to the predicted molecular weight of TRPM8 gene product (M_r 128,000) in COS-7 cells heterologously expressing TRPM8; ref. 2] with or without 1:40 dilution of anti–CD-9 antibody (ref. 10; Dr. Leonie Ashman, University of Adelaide, Australia) at 4°C overnight, and then with

antirabbit IgG secondary antibody conjugated with FITC (1:500 dilution) and antimouse IgG secondary antibody conjugated with Cy3 (1:500 dilution; Jackson ImmunoResearch Laboratories, Inc., West Grove, PA) for 2 hours at room temperature. DiOC6 (Sigma, St. Louis, MO; 1 mmol/L) was used to stain the ER (1 minute at room temperature). Cells were viewed using an Olympus AX70 microscope (Melville, NY) equipped with epifluorescence or attached to a Bio-Rad 1024 scanning confocal system equipped with an argon ion (488 nm) and a helium neon (543 nm) for excitation of FITC or DiOC6, and Cy3, respectively. Confocal images were taken in the equatorial plane. For quantitation, immunofluorescence intensity [arbitrary pixel units (apu)] of each cell was measured using NIH image 1.62.

Measurement of the $[Ca^{2+}]_{cyt}$. Intracellular Ca^{2+} imaging using Fura-2 was conducted as described previously (8). Temperature was controlled by a temperature controller (Cell Microcontrol System, Norfolk, VA) and monitored by a thermistor placed within 160 μm of the field of view. Menthol, thapsigargin, and capsazepine (Sigma) were each applied by superfusion. The rate of Ca^{2+} inflow was determined by measuring the initial slope of the extracellular Ca^{2+} ($Ca^{2+}{}_E$)-induced increase in fluorescence ratio [fluorescence ratio unit (fru)/s; ref. 8]. The amount of Ca^{2+} released from intracellular stores was estimated by calculating the area under the Ca^{2+} release (fru $\times$ s) curve (11). In each case, the difference between the maximal fluorescence ratio value induced by menthol or thapsigargin and the minimum fluorescence ratio value after $[Ca^{2+}]_{cyt}$ had decreased and reached a steady-state value was measured and multiplied by the width of the Ca^{2+} release peak at half height.

Cell Viability and Apoptosis. Cell viability was measured using the MTT (Sigma) test, and apoptotic cells were detected using ethidium bromide (Sigma; ref. 8).

Data Analysis. Results are expressed as mean $\pm$ SE. Statistical analysis was performed using Student's *t* test for unpaired samples. A value of $P < 0.05$ was taken as significant.

RESULTS

Detection of TRPM8 Expression and Its Regulation by Androgen in an Androgen-Sensitive Cell Line. Expression of TRPM8 mRNA in LNCaP cells was detected by reverse transcription-PCR (Fig. 1*A*), thus confirming the results obtained by Tsaveler *et al.* (2). Sequencing confirmed the identity of the 682-bp band with the published TRPM8 sequence (2). Because TRPM8 has been found to coexpress with TRPV1 and ANKTM1 in sensory neurons, the expression of these two channels also was examined (7, 12). However, no mRNA encoding either TRPV1 or ANKTM1 was detected (Fig. 1*A*). Expression of the TRPM8 protein in LNCaP cells was consistently detected by immunofluorescence (Fig. 1, compare *D* with *C*).

To investigate the dependence of TRPM8 expression on androgen, cells were grown for 48 hours in RPMI plus FCS (normal culture medium), in RPMI plus charcoal-stripped FCS (to remove androgen), or in RPMI plus charcoal-stripped FCS supplemented with DHT (0.1 nmol/L; androgen replete medium). The amount of TRPM8 PCR transcript (expressed as a ratio of the amount of GAPDH PCR transcript) in cells grown in RPMI plus FCS was 100 $\pm$ 7.1 aru ($n = 3$). This was decreased to 65.3 $\pm$ 4.5 aru ($n = 3$; $P < 0.01$) in cells incubated in RPMI plus charcoal-stripped FCS but returned to 95.5 $\pm$ 5.8 aru ($n = 3$) in cells grown with DHT (Fig. 1*B*). The mean value of TRPM8 immunofluorescence intensity in cells grown in RPMI plus FCS was 38.4 $\pm$ 7.2 apu per cell (average of 200 to 300 cells from three separate experiments; Fig. 1*E*). This was decreased to 5.7 $\pm$ 1.5 apu ($n = 3$; $P < 0.001$) in cells grown in RPMI plus charcoal-stripped FCS (Fig. 1*F*) after 96 hours but returned to 29.9 $\pm$ 4.9 apu ($n = 3$) in cells grown with DHT (Fig. 1*G*).

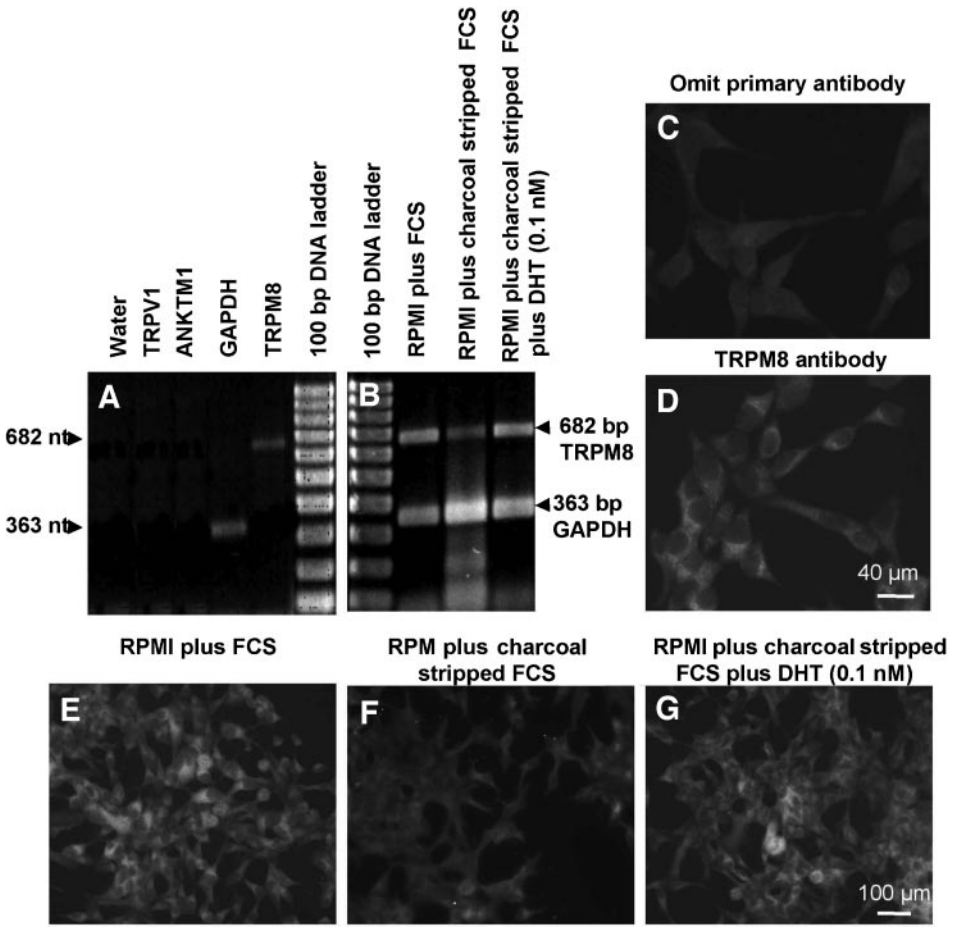

Fig. 1. Regulation of TRPM8 expression by androgen in androgen-responsive LNCaP cells. *A*, reverse transcription-PCR for detection of TRPM8, ANKTM1, TRPV1, and GAPDH using specific primers as described in Materials and Methods. *B*, androgen regulation of TRPM8 mRNA. LNCaP cells were grown for 2 days in RPMI plus FCS (normal culture medium), RPMI plus charcoal-stripped FCS, or in RPMI plus charcoal-stripped FCS with 0.1 nmol/L DHT. RNA was extracted and subjected to reverse transcription-PCR. GAPDH and TRPM8 amplifications were carried out separately using equal amounts of cDNA template from the same sample. PCR products (5 μL) from the two reactions were mixed and subjected to electrophoresis as described in Materials and Methods. Pilot experiments revealed that the amplification of all of the targets remained within the exponential phase. *C* and *D*, detection of TRPM8 in LNCaP cells by immunohistochemistry using an anti-TRPM8 antibody as described in Materials and Methods. *E–G*, androgen regulation of TRPM8 abundance at the protein level. Cells were grown in three different culture media as described in *B*, were fixed after 4 days, and then were subjected to immunohistochemistry. The results are representative of those obtained in three independent experiments.

Intracellular Localization of TRPM8 in an Androgen-Sensitive Cell Line. Using confocal microscopy, the majority of TRPM8 protein was found associated with a reticular structure outside the nucleus (Fig. 2*A* and *D*). Cells were costained with DiOC6 to define the location of the ER (Fig. 2*B*). An antibody against CD-9, located at the PM in LNCaP cells and in a number of other cell types (8, 10), was used as a PM marker. Images of LNCaP cells treated with the anti–CD-9 antibody revealed a clear location of the CD-9 protein at the PM (Fig. 2*E*). Overlay of the TRPM8 and DiOC6 images and the TRPM8 and CD-9 images showed that based on fluorescence intensity, approximately one-half the intracellular TRPM8 protein is colocated with DiOC6 (in the ER; Fig. 2*C*) and approximately one-half is colocated with CD-9 in a band that occupies ~30% to 50% of the PM (indicated by the arrows in Fig. 2*F*).

Increases in $[Ca^{2+}]_{cyt}$ in Response to Cooling and Menthol in an Androgen-Sensitive Cell Line. In the absence of added $Ca^{2+}{}_E$, LNCaP cells exhibited a small increase in Fura II fluorescence ratio ($[Ca^{2+}]_{cyt}$) in response to transient cooling (28°C to 17°C; Fig. 3*A*). $[Ca^{2+}]_{cyt}$ gradually returned to the basal level as the temperature returned to 28°C. A small increase in $[Ca^{2+}]_{cyt}$ was observed when 2 mmol/L Ca^{2+} were added at 28°C (Fig. 3*A*). Of more interest, in the presence of $Ca^{2+}{}_E$, the cells exhibited a remarkable increase in Fura II fluorescence in response to a second round of transient cooling (Fig. 3*A*). In the presence of $Ca^{2+}{}_E$ (at 28°C), menthol(−) (100 mmol/L) induced a substantial increase in $[Ca^{2+}]_{cyt}$ (Fig. 3*B*), with an EC_{50} value of 4.3 ± 1.9 μmol/L (Fig. 3*C*). Another TRPM8 agonist, icilin (1 mmol/L), also induced a substantial increase in $[Ca^{2+}]_{cyt}$ (data not shown). The response to menthol was inhibited 70% by the TRPM8

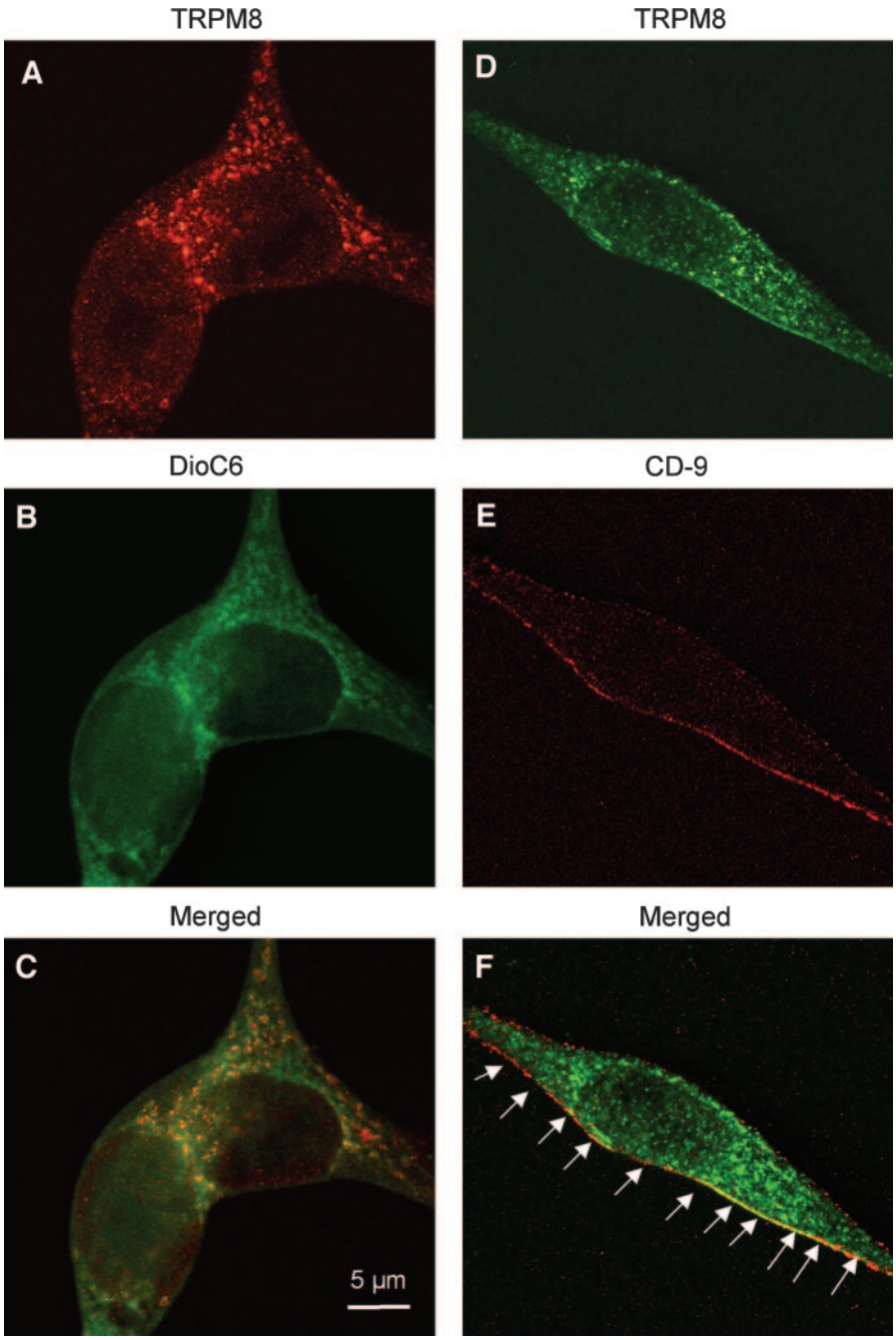

Fig. 2. Intracellular distribution of the TRPM8 protein in androgen-responsive LNCaP cells. *A–C*, a single cell showing TRPM8 immunofluorescence (*A*), DiOC6 fluorescence (*B*), and the merged images (*C*). *D–F*, immunofluorescence images from the same cell of TRPM8 (*D*), the plasma membrane marker protein CD-9 (*E*), and the merged images (F). The arrows (*F*) indicate likely regions of colocalization of TRPM8 and CD-9. DiOC6 fluorescence and immunofluorescence of TRPM8 and CD-9 were determined by confocal microscopy using a 100× objective (zoom threefold). The results shown are representative of those obtained in each of two independent experiments. Results similar to those shown were obtained for 18 of 20 cells examined in one experiment and for 17 of 20 cells examined in the other experiment.

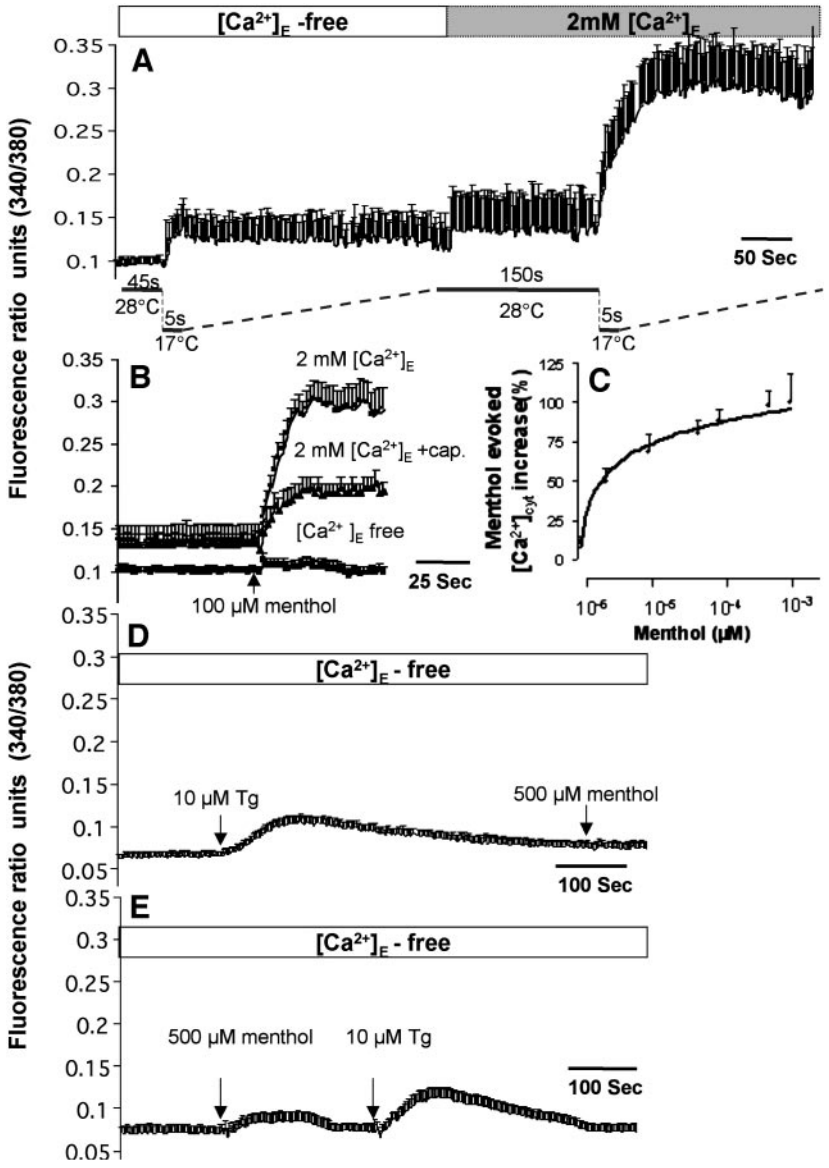

Fig. 3. Increase in $[Ca^{2+}]_{cyt}$ in androgen-responsive LNCaP cells in response to cooling and menthol. *A*. Cooling evoked increases in $[Ca^{2+}]_{cyt}$. Cells were initially incubated in the absence of added $Ca^{2+}{}_E$, and a cool stimulus was applied as indicated. $Ca^{2+}{}_E$ (2 mmol/L) was added at the time indicated by the arrow, followed by another cooling stimulus. The change in bath temperature is represented schematically below the traces. *B*. The menthol(−) induced increase in $[Ca^{2+}]_{cyt}$. Cells were incubated in the absence of added $Ca^{2+}{}_E$ or in the presence of added $Ca^{2+}{}_E$ (2 mmol/L) with and without 10 μmol/L capsazepine (*cap.*). Menthol(−) (100 μmol/L) was added at the time indicated by arrow. *C*, dose-response curve for the menthol(−)-induced increase in $[Ca^{2+}]_{cyt}$. The EC_{50} value was determined as the concentration of test substance required to produce half-maximal increases in $[Ca^{2+}]_{cyt}$. *D*. Cells were incubated in the absence of added $Ca^{2+}{}_E$, and thapsigargin (*Tg*; 10 μmol/L) then was added, followed by menthol (500 μmol/L) as indicated by the arrows. *E*. Cells were incubated in the absence of added $Ca^{2+}{}_E$, and menthol (500 μmol/L) and thapsigargin (10 μmol/L) then were added as indicated by the arrows. $[Ca^{2+}]_{cyt}$ (expressed as fru) was measured as described in Materials and Methods. The results (*A–E*) are representative of one of three experiments (average of 30 to 50 cells) that gave similar results.

antagonist capsazepine (Fig. 3*B*). When tested in the absence of $Ca^{2+}{}_E$, the increase in $[Ca^{2+}]_{cyt}$ evoked by menthol barely was detectable (Fig. 3*B*). These results indicate that the substantial increase in $[Ca^{2+}]_{cyt}$ in response to cooling or menthol is caused by enhanced Ca^{2+} inflow across the PM.

To test whether menthol induces the release of Ca^{2+} from intracellular stores, cells were incubated in the absence of $Ca^{2+}{}_E$, and the effects of menthol were compared with those of thapsigargin (10 μmol/L), an inhibitor of the ER (Ca^{2+} + Mg^{2+})ATPase (13). This concentration of thapsigargin depletes ~95% of the intracellular Ca^{2+} stores (13). Thapsigargin evoked a transient increase in $[Ca^{2+}]_{cyt}$ (Fig. 3*D*), indicating the release of Ca^{2+} from intracellular stores. The amount of Ca^{2+} released was 15.2 ± 3.5 fru × s (n = 3). There was no further detectable $[Ca^{2+}]_{cyt}$ increase when menthol (500 μmol/L) was added after thapsigargin (Fig. 3*D*). Similar results (not shown) were observed with 100 and 1000 μmol/L menthol.

However, when menthol (500 μmol/L) was added before thapsigargin, an increase in $[Ca^{2+}]_{cyt}$ (1.8 ± 0.5 fru × s; n = 3) was observed, followed by another increase with higher magnitude (12.5 ± 1.5 fru × s; n = 3) induced by thapsigargin (Fig. 3*E*).

Menthol-Sensitive Ca^{2+} Influx and Ca^{2+} Store Release Are Regulated by Androgen in an Androgen-Sensitive Cell Line. To test whether androgen regulates TRPM8-mediated Ca^{2+} inflow and Ca^{2+} release, cells were grown in RPMI plus charcoal-stripped FCS for 4 days, and $[Ca^{2+}]_{cyt}$ then was measured in the presence of 2 mmol/L $Ca^{2+}{}_E$. The initial rate of increase in $[Ca^{2+}]_{cyt}$ in response to menthol(−) (100 μmol/L) in cells grown in RPMI plus FCS (normal culture medium) was 41.0 ± 6.7 × 10^{-5} fru × s (n = 3). This was reduced to 9.5 ± 1.5 × 10^{-5} fru/s (n = 3; $P < 0.001$) in cells grown in RPMI plus charcoal-stripped FCS but was restored to 32.8 ± 5.5 × 10^{-5} fru/s (n = 3) for cells grown in the presence of DHT. The amount of Ca^{2+} released by menthol(−) (500 μmol/L) in cells incubated in the absence of added $Ca^{2+}{}_E$ was 1.6 ± 0.3 fru × s (n = 3) in cells grown in RPMI plus FCS. This was decreased to 0.11 ± 0.1 fru × s ($P < 0.001$; n = 3) for cells grown in RPMI plus charcoal-stripped FCS. No significant decrease was observed in thapsigargin-induced Ca^{2+} release measured in the absence of added $Ca^{2+}{}_E$ in cells grown in RPMI plus charcoal-stripped FCS (10.8 ± 1.2 fru × s; n = 3) when compared with cells grown in RPMI plus FCS (13 ± 1.8 fru × s; n = 3).

Expression of TRPM8 in an Androgen-Insensitive Cell Line. The expression of TRPM8 in the PC-3 androgen-insensitive cell line also was investigated. Immunocytochemistry using the TRPM8 antibody showed that TRPM8 was detected in PC-3 cells (Fig. 4, compare *B* with *A*). The other interesting finding was that TRPM8 immunofluorescence was clearly seen on plasma membrane in ~20% of all of the PC-3 cells examined (Fig. 4*E*). Those cells that exhibited TRPM8 immunofluorescence at the plasma membrane usually were large and exhibited polymorphism.

Although the level of TRPM8 immunofluorescence intensity was significantly reduced when the cells were grown for 48 hours in RPMI plus charcoal-stripped FCS compared with those in RPMI plus FCS, incubation of cells with DHT (0.1 nmol/L) did not alter the level of TRPM8 expression (Fig. 4*B–D*). The mean values of TRPM8 immunofluorescence intensity in cells grown in RPMI plus FCS (Fig. 4*B*), RPMI plus charcoal-stripped FCS (Fig. 4*C*), and RPMI plus charcoal-stripped FCS in the presence of DHT (Fig. 4*D*) were 25.7 ± 2.0, 15.3 ± 1.9, and 16.9 ± 2.4 apu (average of 200 to 300 cells from two separate experiments), respectively.

Evidence for functional expression of TRPM8 in PC-3 cells was obtained using Ca^{2+} imaging and menthol. For PC-3 cells incubated in the presence of 2 mmol/L $Ca^{2+}{}_E$, a high concentration of menthol (1000 μmol/L) induced a small increase in $[Ca^{2+}]_{cyt}$ (Fig. 4*F*). These results indicate that TRPM8 is expressed at a low level in PC-3 cells, but its expression in these cells is not regulated by androgen.

Capsazepine Reduces the Survival of Androgen-Sensitive Cells by Induction of Apoptosis. To test whether the androgen-regulated TRPM8 Ca^{2+}-permeable channel is coupled with Ca^{2+} and other signaling pathways involved in cell survival (14, 15), LNCaP cells were incubated with capsazepine for 3 days, and nuclear morphology and cell viability then were examined. Cells grown in RPMI plus FCS with 10 μmol/L capsazepine exhibited nuclear condensation and fragmentation (Fig. 5, compare *C* with *A*), whereas cells grown in RPMI plus charcoal-stripped FCS (to down-regulate expression of TRPM8) with 10 μmol/L capsazepine did not (Fig. 5, compare *D* with *B*). The percentage of viable cells, assessed using the MTT test, in cultures of capsazepine-treated cells was significantly decreased compared with that of cells grown under normal conditions (Fig. 5*E*). In

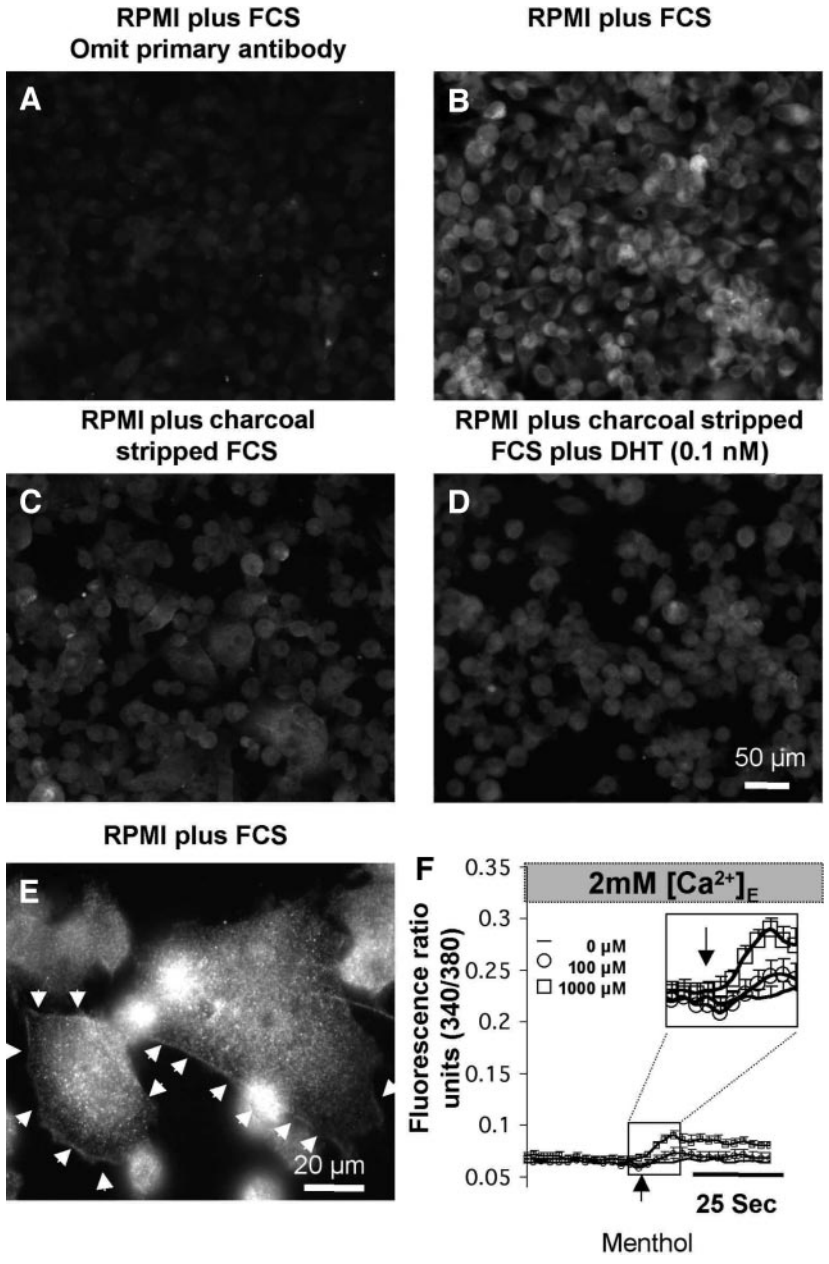

Fig. 4. Expression and intracellular distribution of TRPM8 in androgen-insensitive PC-3 cells. *A–E*, immunofluorescence images of TRPM8 in PC-3 cells incubated in RPMI plus FCS (*B* and *E*), RPMI plus charcoal-treated FCS (*C*), RPMI plus charcoal-treated FCS in the presence of 0.1 nmol/L DHT (*D*), and in RPMI plus FCS but with the omission of the primary antibody (control; *A*). *E,* TRPM8 immunofluorescence image at higher magnification, showing the presence of TRPM8 at the plasma membrane (*arrows*) and intracellular sites. The results (*A–E*) are representative of one of two experiments (average, 200 to 300 cells) that gave similar results. *F*, menthol(−)-induced increase in $[Ca^{2+}]_{cyt}$. Cells were incubated in the presence of 2 mmol/L $Ca^{2+}{}_E$, and menthol(−) (100 or 1000 μmol/L as indicated) was added at the time indicated by the arrow. The results shown are the mean ± SE of one of two experiments (average of 30 cells) that gave similar results.

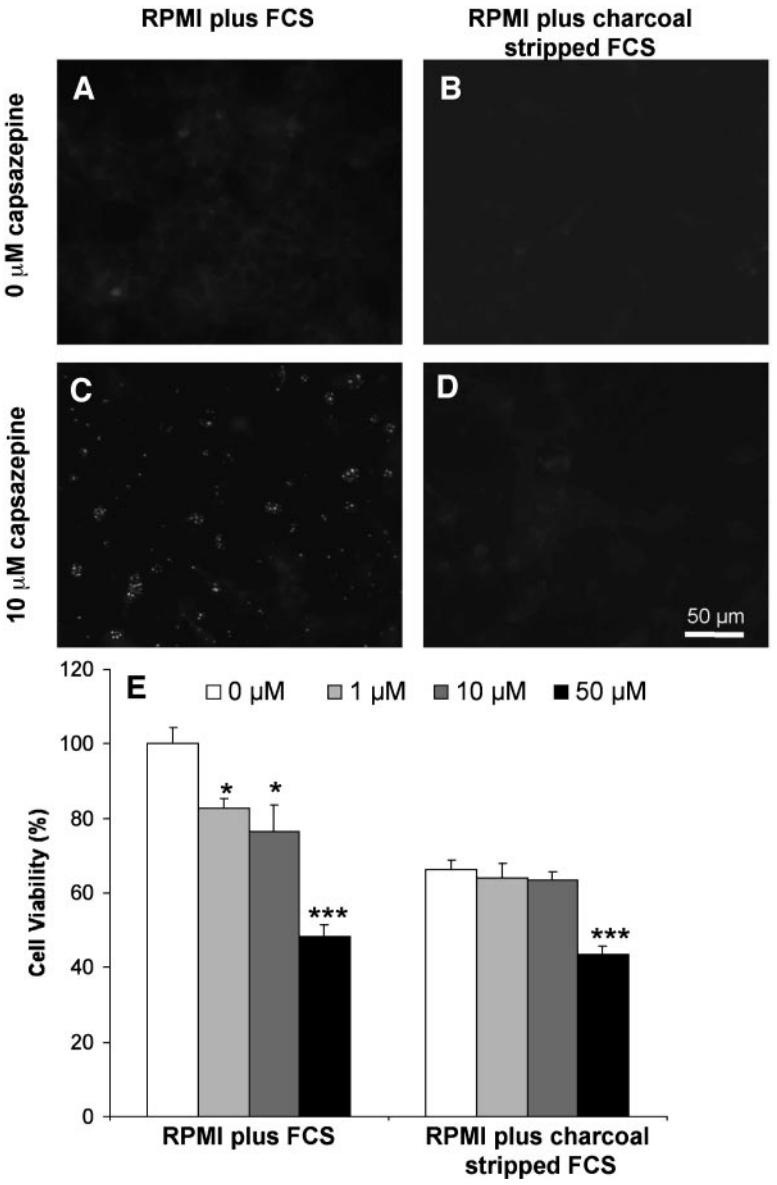

Fig. 5. Capsazepine induces apoptosis and reduces the survival of androgen-sensitive LNCaP cells. *A–D*. Cells grown for 4 days in RPMI plus FCS (normal culture conditions; *A* and *C*) and in RPMI plus charcoal-stripped FCS (*B*, *D*) then were incubated with 0 (*A*, *B*) and 10 μmol/L (*C*, *D*) capsazepine for an additional 3 days. Nuclear morphology was assessed using ethidium bromide as described in Materials and Methods. The results shown are representative of one of three experiments that gave similar results. *E*. Cell viability was assessed using the MTT test in cells treated with 1, 10, and 50 μmol/L capsazepine for 3 days as described in Materials and Methods; $*P < 0.05$, $***P < 0.001$. Cells treated with capsazepine were compared with cells treated with vesicle control under the same culture conditions. The results shown are the average of three independent experiments.

contrast, when cells were grown in RPMI plus charcoal-stripped FCS, those treated with 1 and 10 μmol/L capsazepine retained viability, whereas those incubated with 50 μmol/L capsazepine exhibited decreased viability (Fig. 5*E*).

Small Interference RNA against TRPM8 Reduces the Survival of Androgen-Sensitive Cells by Induction of Apoptosis. Experiments using siRNA were carried out to further clarify the role of TRPM8 in the survival of LNCaP cells. The siRNA targeted against TRPM8 down-regulated TRPM8 protein expression ~50% compared with the effects of negative control siRNA, TRPM8 antisense RNA, and nontransfected cells (Fig. 6*A–C*). A significant reduction in the percentage of viable cells was observed in cells transfected with TRPM8 siRNA (Fig. 6*F*). Staining the nucleus revealed a large number of apoptotic nuclei (Fig. 6, compare *E* with *D*). Therefore, the results further confirm that TRPM8 is important for the survival of LNCaP cells.

Effect of Menthol on the Viability of Androgen-Sensitive Cells. We also tested the effect of menthol on the viability of LNCaP cells. Because menthol activates TRPM8, which in turn leads to a sustained inflow of Ca^{2+} in LNCaP cells (Fig. 3*B*), and because it has been shown that a sustained inflow of Ca^{2+} to cells through some Ca^{2+}-permeable channels that are members of the TRP family leads to cell death (16, 17), it was predicted that menthol would induce cell death in LNCaP cells. Incubation of LNCaP cells with menthol for 3 days reduced by half the percentage of viable cells (Fig. 7*A*) and increased the number of cells exhibiting apoptotic nuclei (Fig. 7, compare *C* with *B*).

DISCUSSION

The immunofluorescence results show that the TRPM8 protein is clearly expressed in androgen-responsive LNCaP cells. TRPM8 was found at the ER and at the PM. The following observations provide evidence that the Ca^{2+} inflow and Ca^{2+} release from intracellular stores are mediated by TRPM8: (*a*) Ca^{2+} movement was activated by cooling and menthol, known activators of heterologously expressed TRPM8 (4, 5); (*b*) capsazepine, a known antagonist of TRPM8 (18), blocked the actions of menthol; and (*c*) the concentration of menthol that gave half-maximal activation of the Ca^{2+} fluxes, and the concentrations of capsazepine that inhibited menthol-stimulated Ca^{2+} inflow are in the range shown by others (18) to affect heterologously expressed TRPM8. Although capsazepine also is known to block

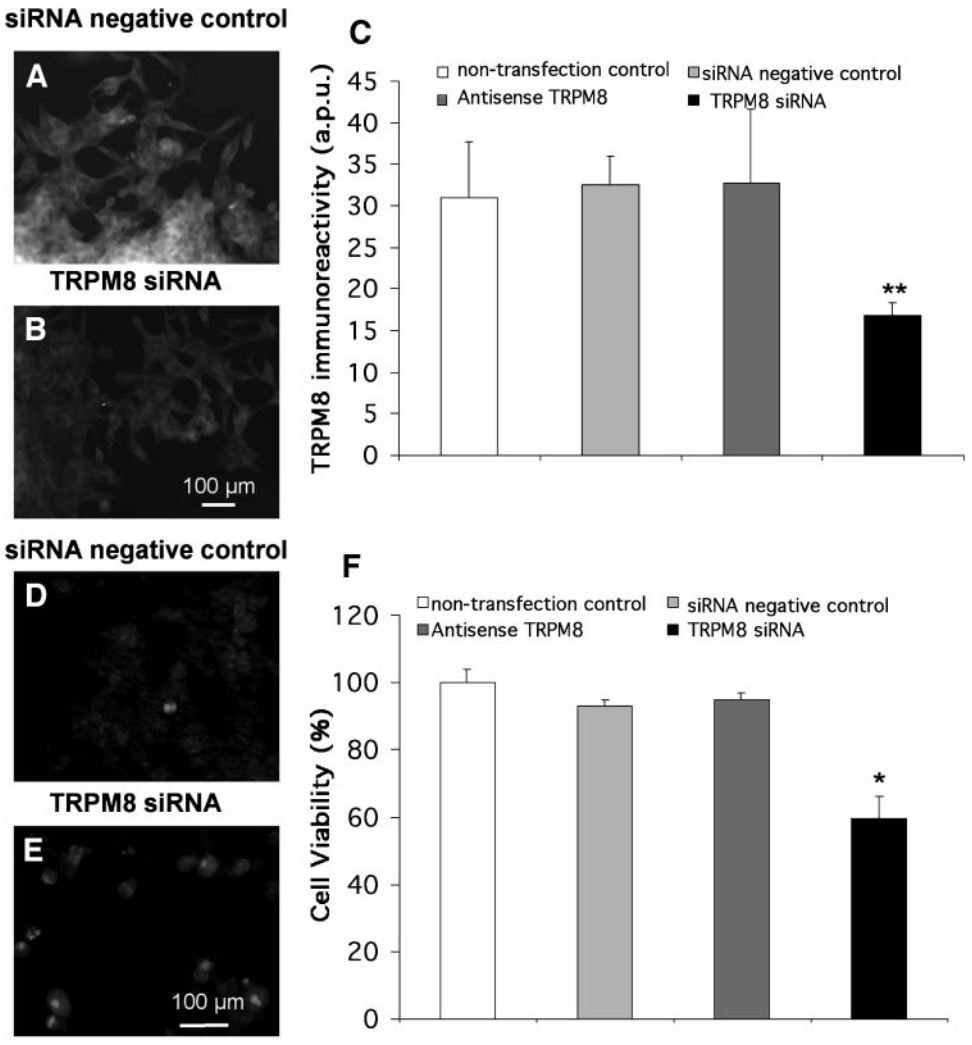

Fig. 6. Suppression of TRPM8 expression by siRNA targeted against TRPM8 reduces the percentage of viable androgen-sensitive LNCaP cells and induces apoptosis. *A* and *B*, immunofluorescence images of cells treated with a negative control siRNA (20 nmol/L; *A*) and siRNA targeted to TRPM8 (20 nmol/L; *B*). *C*, histogram showing the effect of siRNAs on expression of TRPM8; mean ± SE of two experiments; $^{**}P < 0.01$. *D* and *E*, fluorescence images of LNCaP cells stained with ethidium bromide after transfection with negative control (*D*) or TRPM8 (*E*) siRNA. *F*, histogram of percentage of viable cells (determined using the MTT assay) after transfection with a given siRNA species; mean ± SE of two experiments; $^{*}P < 0.05$.

TRPV1 (19), the involvement of TRPV1 in mediating the observed Ca^{2+} fluxes can be excluded because no TRPV1 mRNA was detected in LNCaP cells.

Whereas cooling and menthol induced a small increase in $[Ca^{2+}]_{cyt}$ in LNCaP cells incubated in the absence of $Ca^{2+}{}_{E}$, these increases in $[Ca^{2+}]_{cyt}$ were much smaller than those observed in cells incubated in the presence of $Ca^{2+}{}_{E}$. Moreover, a much higher concentration of menthol was required to cause a detectable increase in $[Ca^{2+}]_{cyt}$ in the absence of $Ca^{2+}{}_{E}$, and the effect of menthol was considerably smaller than that of thapsigargin. These results indicate that although cooling and menthol induce the release of some Ca^{2+} from intracellular stores, the predominant effect is the activation of Ca^{2+} inflow. It is possible that Ca^{2+} inflow through store-operated Ca^{2+}channels (activated by the decrease in $[Ca^{2+}]$ in the ER induced by the effect of cooling or menthol on TRPM8 in the ER) makes some contribution to the observed Ca^{2+} inflow initiated by cooling and menthol. The action of cooling and menthol in stimulating Ca^{2+} fluxes across the PM and the ER membrane is consistent with the intracellular location of the TRPM8 protein at these two sites.

The activation by menthol of TRPM8 located at intracellular sites requires that menthol can move into the cytoplasmic space. Several studies provide indirect evidence that cell membranes are permeable to menthol. Thus, it has been shown that menthol increases the transdermal and transbuccal absorption of drugs by affecting intracellular lipids and proteins (20, 21) and inhibits arylamine *N*-acetyltransferase activity in human liver tumor cells (22). These results, as well as the knowledge that menthol is lipid soluble (20, 21), suggest that it is likely menthol can diffuse from the extracellular space to intracellular TRPM8 locations.

Our results clearly show that androgen increases and the absence of androgen decreases TRPM8 protein expression and Ca^{2+} flow across the PM and ER mediated by TRPM8 in an androgen-responsive cell line. We looked for putative androgen response elements based on the consensus androgen-response element AGAACAnnnTGTTCT (9) in the regulatory region of the human *TRPM8* gene (2). One putative androgen-response element was identified in the 5′ flank region of *TRPM8* gene that is close to the transcription start site (−242; Fig. 8). Eleven putative androgen-response elements were identified in introns of the *TRPM8* gene. In particular, in introns 3 and 22, two androgen-response elements with high homology with the TRANSFAC consensus androgen-response element motif (11 of 12, 92%, of nucleotides were identical) were detected (Fig. 8). These putative androgen-response elements may confer the inducibility of *TRPM8* gene expression by androgen at transcription level in prostate cells.

Expression of the TRPM8 protein also was detected in the androgen-unresponsive PC-3 prostate cancer cell line. Although menthol caused an increase in $[Ca^{2+}]_{cyt}$ in these cells (in the presence of $Ca^{2+}{}_{E}$), the effect was small compared with that in LNCaP cells. Incubation of PC-3 cells in RPMI plus charcoal-stripped FCS (designed to remove endogenous androgens) decreased TRPM8 immu-

nofluorescence, but there was no response to added DHT. These results indicate that, as expected for an androgen-unresponsive cell line, expression of TRPM8 did not respond to androgen. The decrease in TRPM8 protein expression observed in cells incubated in RPMI plus charcoal-treated FCS might have been caused by the removal of other factors (*e.g.,* growth factors) from the FCS by the charcoal treatment (23).

Capsazepine, at concentrations in the range that are known to inhibit the activation of heterologously expressed TRPM8 (18), and suppression of TRPM8 expression with siRNA each increased the number of androgen-responsive LNCaP cells undergoing apoptosis and decreased cell viability. These observations indicate that the normal function of TRPM8 is required for LNCaP cell survival. The concentration of capsazepine that reduced the percentage of viable cells by ~50% was ~50 μmol/L. This is within the range of 20 μmol/L reported for the concentration of capsazepine that gives 50% inhibition of TRPM8 heterologously expressed in HEK-293 cells (18). Although an effect of capsazepine on TRPV1 can be excluded, as argued previously, the possibility that the capsazepine-induced decrease in cell viability is caused by the action of capsazepine on a protein(s) other than TRPM8 cannot be completely excluded (24). However, the observation that the effect of capsazepine in reducing cell viability is considerably decreased in cells incubated in RPMI plus charcoal-stripped FCS (androgen-deprived medium; in which expression of TRPM8 also is considerably decreased) provides additional evidence that the effect of capsazepine is via inhibition of the TRPM8 channel.

If TRPM8 is proposed to be necessary for cell survival and if TRPM8 expression is reduced in LNCaP cells incubated in RPMI plus charcoal-stripped FCS, it might be predicted that capsazepine would have a greater effect in reducing the percentage of viable cells when LNCaP cells are grown in RPMI plus charcoal-stripped FCS. However, this was not observed (Fig. 5*E*). This is likely because of differences in the culture medium and the effects of growth in RPMI plus charcoal-stripped FCS *per se* (23). Thus, the initial culture conditions (FCS compared with charcoal-stripped FCS) are different, as indicated by the observation that in the absence of capsazepine, the percentage of viable cells present in RPMI plus charcoal-stripped FCS is only 60% of that in RPMI plus FCS (normal medium).

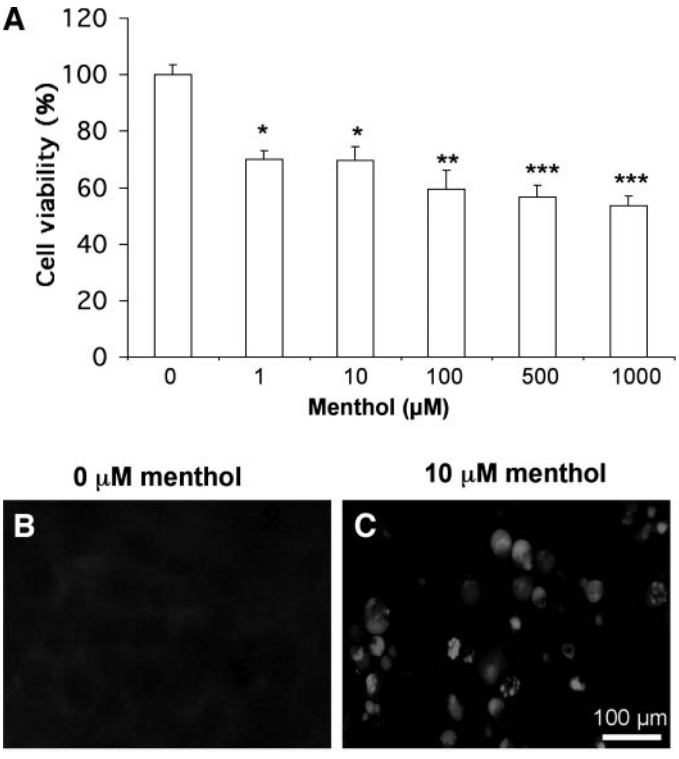

Fig. 7. Menthol reduces the percentage of viable cells and induces apoptosis in androgen-sensitive LNCaP cells. *A*, histogram of the percentage of viable cells observed in the presence and absence of the indicated concentrations of menthol; mean ± SE of two experiments; $*P < 0.05$, $**P < 0.01$, and $***P < 0.001$. *B* and *C*, fluorescence images of cells showing nuclear DNA fragmentation revealed by ethidium bromide in the presence (*C*) and absence (*B*) of incubation for 3 days in the presence of 100 μmol/L menthol. The results are representative of one of two experiments that gave similar results.

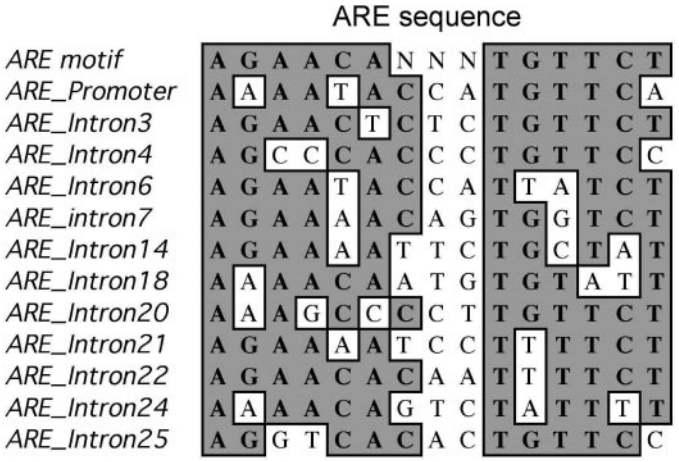

Fig. 8. Putative androgen-response elements identified by searching the 5′ regulatory regions and introns of human *TRPM8* gene for a motif corresponding to the TRANSFAC androgen-response element consensus sequence, AGAACAnnnTGTTCT (*ARE*). A ClustalW alignment identifies conserved residues in gray.

Menthol decreased the percentage of viable cells and increased the number of cells undergoing apoptosis in LNCaP cells cultured in RPMI plus FCS (normal medium that contains 2 mmol/L $Ca^{2+}{}_E$). Because menthol was shown to cause a sustained increase in $[Ca^{2+}]_{cyt}$ in LNCaP cells, it is likely that menthol-induced cell death is mediated at least in part by the sustained increase in $[Ca^{2+}]_{cyt}$. This likely represents a pathophysiologic action of TRPM8 (the channel would not normally be activated in a sustained manner) as compared with a normal role in cell survival as revealed by the experiments with capsazepine and TRPM8 siRNA.

Considering the normal physiologic function of TRPM8, it recently has been suggested that TRPM8 serves as a cold sensor in the prostate (25). TRPM8 also may be involved in other functions such as the regulation of proliferation and/or apoptosis (and hence the control of cell number) and in ion and protein secretion in prostate epithelial cells. One interesting possibility comes from the recent observation that geraniol activates TRPM8 (18). The PP_i ester of geraniol is an intermediate in cholesterol synthesis (26), and geraniol enhances cell proliferation in prostate epithelium (27). Thus, it is possible that in prostate epithelial cells, TRPM8 is involved in the regulation of cell proliferation and responds to geraniol as an intracellular messenger.

ACKNOWLEDGMENTS

We thank Mrs. Diana Kassos for typing the manuscript and Mrs. Rachael Hughes for assistance with cell culture.

REFERENCES

1. Parker SL, Tong T, Bolden S, Wingo PA. Cancer statistics. CA Cancer J Clin 1996;46:5–27.
2. Tsavaler L, Shapero MH, Morkowski S, Laus R. Trp-p8, a novel prostate-specific gene, is up-regulated in prostate cancer and other malignancies and shares high homology with transient receptor potential calcium channel proteins. Cancer Res 2001;61:3760–9.

3. Henshall SM, Afar DE, Hiller J, et al. Survival analysis of genome-wide gene expression profiles of prostate cancers identifies new prognostic targets of disease relapse. Cancer Res 2003;63:4196–203.
4. McKemy DD, Neuhausser WM, Julius D. Identification of a cold receptor reveals a general role for TRP channels in thermosensation. Nature 2002;416:52–8.
5. Peier AM, Moqrich A, Hergarden AC, et al. A TRP channel that senses cold stimuli and menthol. Cell 2002;108:705–15.
6. Thut PD, Wrigley D, Gold MS. Cold transduction in rat trigeminal ganglia neurons in vitro. Neuroscience 2003;119:1071–83.
7. Zhang L, Jones S, Brody K, Costa M, Brookes SJ. Thermosensitive transient receptor potential channels in vagal afferent neurons of the mouse. Am J Physiol Gastrointest Liver Physiol 2004;286:G983–91.
8. Zhang L, Brereton HM, Hahn M, et al. Expression of Drosophila Ca^{2+} permeable transient receptor potential-like channel protein in a prostate cancer cell line decreases cell survival. Cancer Gene Ther 2003;10:611–25.
9. Nelson PS, Clegg N, Arnold H, et al. The program of androgen-responsive genes in neoplastic prostate epithelium. Proc Natl Acad Sci USA 2002;99:11890–5.
10. Imamura N, Mtasiwa DM, Ota H, Inada T, Kuramoto A. Distribution of cell surface glycoprotein CD9 (P24) antigen on megakaryocyte lineage leukemias and cell lines. Am J Hematol 1990;35:65–7.
11. Wang YJ, Gregory RB, Barritt GJ. Maintenance of the filamentous actin cytoskeleton is necessary for the activation of store-operated Ca^{2+} channels, but not other types of plasma-membrane Ca^{2+} channels, in rat hepatocytes. Biochem J 2002;363:117–26.
12. Story GM, Peier AM, Reeve AJ, et al. ANKTM1, a TRP-like channel expressed in nociceptive neurons, is activated by cold temperatures. Cell 2003;112:819–29.
13. Thastrup O, Cullen PJ, Drobak BK, Hanley MR, Dawson AP. Thapsigargin, a tumor promoter, discharges intracellular Ca^{2+} stores by specific inhibition of the endoplasmic reticulum $Ca^{2(+)}$-ATPase. Proc Natl Acad Sci USA 1990;87:2466–70.
14. Gutierrez AA, Arias JM, Garcia L, Mas-Oliva J, Guerrero-Hernandez A. Activation of a Ca^{2+}-permeable cation channel by two different inducers of apoptosis in a human prostatic cancer cell line. J Physiol 1999;517:95–107.
15. Furuya Y, Lundmo P, Short AD, Gill DL, Isaacs JT. The role of calcium, pH, and cell proliferation in the programmed (apoptotic) death of androgen-independent prostatic cancer cells induced by thapsigargin. Cancer Res 1994;54:6167–75.
16. Yoon J, Ben-Ami HC, Hong YS, et al. Novel mechanism of massive photoreceptor degeneration caused by mutations in the trp gene of Drosophila. J Neurosci 2000; 20:649–59.
17. Aarts M, Iihara K, Wei WL, et al. A key role for TRPM7 channels in anoxic neuronal death. Cell 2003;115:863–77.
18. Behrendt HJ, Germann T, Gillen C, Hatt H, Jostock R. Characterization of the mouse cold-menthol receptor TRPM8 and vanilloid receptor type-1 VR1 using a fluorometric imaging plate reader (FLIPR) assay. Br J Pharmacol 2004;141:737–45.
19. Caterina MJ, Schumacher MA, Tominaga M, Rosen TA, Levine JD, Julius D. The capsaicin receptor: a heat-activated ion channel in the pain pathway. Nature 1997; 389:816–24.
20. Jain AK, Thomas NS, Panchagnula R. Transdermal drug delivery of imipramine hydrochloride. I. Effect of terpenes. J Control Release 2002;79:93–101.
21. Shojaei AH, Khan M, Lim G, Khosravan R. Transbuccal permeation of a nucleoside analog, dideoxycytidine: effects of menthol as a permeation enhancer. Int J Pharm 1999;192:139–46.
22. Lin JP, Li YC, Lin WC, Hsieh CL, Chung JG. Effects of (−)-menthol on arylamine N-acetyltransferase activity in human liver tumor cells. Am J Chin Med 2001;29:321–9.
23. McBride JH, Davies RJ. Adsorbent treatment and immunoaffinity chromatography compared for removing estradiol-17 ā from plasma. Clin Chem 1981;27:612–4.
24. Ray AM, Benham CD, Roberts JC, et al. Capsazepine protects against neuronal injury caused by oxygen glucose deprivation by inhibiting I(h). J Neurosci 2003;23:10146–53.
25. Stein RJ, Santos S, Nagatomi J, et al. Cool (TRPM8) and hot (TRPV1) receptors in the bladder and male genital tract. J Urol 2004;172:1175–8.
26. Voet D, Voet JG. Biochemistry. New York: John Wiley & Sons; 1990.
27. Paubert-Braquet M, Cousse H, Raynaud JP, Mencia-Huerta JM, Braquet P. Effect of the lipidosterolic extract of Serenoa repens (Permixon) and its major components on basic fibroblast growth factor-induced proliferation of cultures of human prostate biopsies. Eur Urol 1998;33:340–7.